

Nonmagnetic impurities in spin-gapped and gapless Heisenberg antiferromagnets

A. W. Sandvik* and E. Dagotto

National High Magnetic Field Laboratory, Florida State University, 1800 East Paul Dirac Drive, Tallahassee, Florida 32306

D. J. Scalapino

Department of Physics, University of California, Santa Barbara, California 93106

(Received 18 February 1997; revised manuscript received 30 May 1997)

We discuss the effects of nonmagnetic impurities (static holes) in the $S=1/2$ Heisenberg model on a two-dimensional (2D) square lattice, and on two- and three-leg ladders. Results of quantum Monte Carlo simulations show that a *free* localized moment is induced around an isolated impurity only in the spin-gapped two-leg ladder, in agreement with previous theoretical expectations. The localization length of the $S=1/2$ impurity moment in a two-leg ladder with isotropic couplings is ≈ 1.5 lattice spacings. In gapless ladders (odd number of legs) and in the 2D lattice, no free moments are induced. However, in the 2D system, which has antiferromagnetic long-range order at $T=0$ and a gap for longitudinal fluctuations, the impurity leads to a localized distortion of the magnetization in the direction of the broken symmetry, with total $S^z=1/2$. The shape of the distortion is in close agreement with previous spin-wave calculations. For all the systems, a *staggered* moment is induced by the impurity. For the gapped two-leg ladder this is exponentially localized within a length equal to the spin correlation length of the ladder (≈ 3.2 lattice spacings). For the three-leg ladder, the integrated staggered moment diverges as the system size goes to infinity, but the staggered magnetization at a given site appears to vanish. In 2D, we discuss the behavior seen in finite systems both with and without additional symmetry-breaking mechanisms. We also discuss the effect of impurities on the NMR Knight shift and the bulk magnetic susceptibility. [S0163-1829(97)00541-9]

I. INTRODUCTION

Nonmagnetic impurities introduced into various cuprate material alter their magnetic properties in ways which reflect the nature of the correlations in the pure systems. Experimentally, Mahajan *et al.*¹ have used the ^{89}Y NMR response to study the effect of Zn impurities on surrounding Cu spins in $\text{YBa}_2(\text{Cu}_{1-y}\text{Zn}_y)\text{O}_{6+x}$ for various amounts of oxygen. Azuma *et al.*² have studied the case of Zn impurities substituted for Cu in the two-leg and three-leg spin-1/2 Heisenberg ladder materials $\text{Sr}_2(\text{Cu}_{1-y}\text{Zn}_y)_2\text{O}_3$ and $\text{Sr}_2(\text{Cu}_{1-y}\text{Zn}_y)_3\text{O}_5$. If the Zn impurity maintains a nominal Cu^{2+} charge, the Zn^{2+} would have a $(3d)^{10}$, $S=0$ configuration and act as a nonmagnetic impurity. Thus an interesting question is whether a nonmagnetic impurity can induce a local moment on the surrounding Cu^{2+} sites. In the fully oxidized YBCO₇ material, the induced moment was found to be small, of order $0.2\mu_B$ per Zn, while it was of order $0.8\mu_B$ per Zn for an oxygen reduced sample which exhibited a spin gap. This was in approximate agreement with theoretical expectations that a nonmagnetic impurity can only induce a local moment when the mother phase has a spin gap.³ From this point of view, one would expect that in spin-gapped antiferromagnetic two-leg ladders, Zn impurities would create local moments, while in three-leg ladders they would not. However, the initial experiments on the two- and three-leg ladders found that comparable local moments were introduced in both of these systems. Here we use numerical techniques to investigate the problem of induced moments around nonmagnetic impurities in the Heisenberg model on a two-dimensional (2D) square lattice, as well as in two- and three-leg ladders.

The Hamiltonian for the various lattices that we study is the standard Heisenberg model with nearest-neighbor interactions

$$\hat{H} = J \sum'_{\langle i,j \rangle} \mathbf{S}_i \cdot \mathbf{S}_j, \quad (1)$$

where $\langle i,j \rangle$ denotes a pair of nearest-neighbor sites on a square lattice with $n \times L$ sites ($n=2,3,L$), and the primed sum excludes impurity sites. Here we focus primarily on the problem of the magnetic correlations around a single nonmagnetic impurity, and only comment on some aspects of the case of a finite impurity concentration. We use a finite-temperature quantum Monte Carlo (QMC) technique based on a power series expansion of the operator $\exp(-\beta\hat{H})$, where β is the inverse temperature J/T ("stochastic series expansion").⁴ This technique is an improved variant of the so-called Handscomb technique,⁵ and is free from systematic errors of the "Trotter breakup" used in standard worldline methods.⁶ Low enough temperatures can be reached for obtaining ground state results for lattices with up to hundreds of sites. The method has recently been applied to a variety of spin problems.⁷

The outline of the rest of the paper is as follows. In Sec. II we calculate the magnetization distribution around isolated impurities at $T=0$. Finite-size scaling of results for the different types of lattices are used to determine whether or not localized moments are formed. In Sec. III we discuss the effects of impurities on the NMR Knight shift at finite T . In Sec. IV we discuss systems with a finite concentration of impurities, in particular the effects on the bulk susceptibility. We summarize our study in Sec. V.

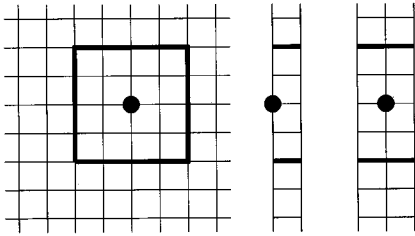


FIG. 1. Illustration of the different lattices with a single spin at $(x,y)=(0,0)$ removed (indicated by the solid circles). The bold lines indicate sites at a frame distance $R=2$ from the impurity.

II. MAGNETIZATION DISTRIBUTION AND LOCALIZED MOMENTS

In this section the magnetization distribution at $T=0$ is investigated for systems with a single impurity. For a bipartite lattice with an even number of sites, removing one spin leads to a ground state with $S=1/2$.⁸ The ground state is hence twofold degenerate, with $m^z = \pm 1/2$. Choosing one of these states, one can calculate the position dependent magnetization $\langle S^z(x,y) \rangle$. The behavior of this quantity as a function of the distance from the impurity site gives direct information on whether or not a moment is formed.

Here we will present numerical results for two- and three-leg ladders, as well as 2D systems. Figure 1 illustrates the different lattices with an impurity at $(x,y)=(0,0)$. For the ladders, the x and y directions are defined as the rung and chain directions, respectively. We use periodic boundary conditions in both directions in the 2D case, and in the chain direction of the ladders. The QMC calculations were carried out at temperatures low enough for thermal expectation values to be completely dominated by the ground state. Typically, inverse temperatures $\beta \approx L, 2L, \text{ and } 4L$ were used for the two-leg ladders, three-leg ladders, and 2D lattices, respectively. Comparing with results at higher temperatures, we find that there are only very minor contributions of excited states in the low- T results discussed here.

For the discussion of the magnetization distribution we define the ‘‘frame distance’’ R from the impurity as indicated in Fig. 1. The total uniform (0) and staggered (π) magnetizations of frame R are defined according to

$$M_0(R) = \sum_{r(x,y)=R} \langle S^z(x,y) \rangle, \quad (2a)$$

$$M_\pi(R) = \sum_{r(x,y)=R} (-1)^{x+y} \langle S^z(x,y) \rangle, \quad (2b)$$

where $r(x,y)$ is the frame distance between the impurity and the site at (x,y) . We also define the total magnetizations within distance R :

$$I_{0,\pi}(R) = \sum_{R' \leq R} M_{0,\pi}(R'). \quad (3)$$

For a system with a localized $S=1/2$ moment, $I_0(R)$ should approach $1/2$ exponentially fast as $R \rightarrow \infty$. Equivalently, for a given distance R close to the impurity, $I_0(R)$ should approach a finite value as the system size goes to infinity. On the other hand, if no moment is formed, the magnetization is

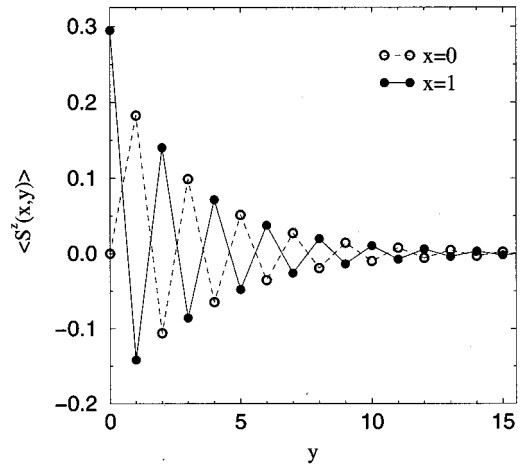


FIG. 2. The average magnetization vs the distance from the impurity for a two-leg ladder of length $L=64$. Open circles are for sites on the same leg ($x=0$) as the impurity, and solid circles for sites on the chain across the impurity ($x=1$).

spread over the system, and as the system size grows one will observe that for a fixed R , $I_0(R) \rightarrow 0$. We use the staggered quantity $I_\pi(R)$ in a similar manner to determine whether a staggered moment is induced. Since the staggered magnetization is not a conserved quantity, the size of a staggered moment can be arbitrary.

A. Two-leg ladders

We begin by discussing the two-leg ladder,^{9–11} in which a localized moment is expected to be induced, on account of the pure system being gapped.³ Figure 2 shows the magnetization $\langle S^z(x,y) \rangle$ vs the distance from the impurity for a 2×64 system. The magnetization is largest at the site on the same rung as the impurity, and has a rapidly decaying oscillating behavior versus the distance from the impurity. Figure 3 shows the integrated uniform and staggered magnetizations vs R for systems of linear sizes $L=16, 32, \text{ and } 64$, with R defined in Fig. 1. There are only very minor differences in $I_0(R)$ for the different lattice sizes, and the approach to the full magnetization $1/2$ is exponential. A line fit to $\ln[M_0(R)]$ for $R \geq 3$ gives a localization length $\xi_0 \approx 1.5$ lattice spacings. The induced staggered magnetization $M_\pi(R)$ has a localization length $\xi_\pi \approx 3.2$, consistent with the spin correlation length of the pure ladder.¹⁰ The ratio $\xi_\pi/\xi_0 \approx 2$ is consistent with the ratio of the gaps of the pure ladder at the corresponding momenta $\mathbf{k}=(0,0)$ and $\mathbf{k}=(\pi,\pi)$.¹¹ The total staggered moment $I_\pi(R \rightarrow \infty) \approx 2.8$.

B. Three-leg ladders

Ladders with an odd number of legs are gapless, and a uniform moment is therefore not expected to form around an impurity.³ The low-energy properties of the three-leg ladder maps onto those of the spin- $1/2$ chain.¹² One might then expect the case of a static impurity to correspond to a spin- $1/2$ chain with a defect. Eggert and Affleck used conformal field theory to study various defects in spin- $1/2$ chains, and concluded that in most cases defects are screened and the fixed point is a chain with open boundary conditions.¹³ How-

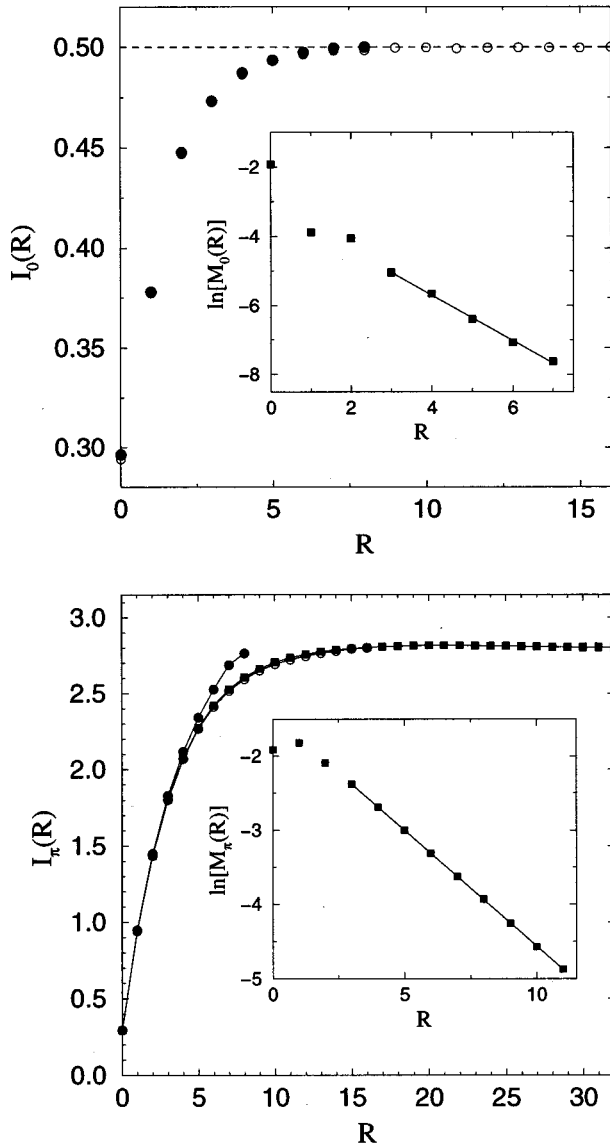


FIG. 3. The integrated uniform (top panel) and staggered (bottom panel) magnetizations vs the distance from the impurity (with R defined in Fig. 1) for two-leg ladders of length $L=16$ (solid circles), 32 (open circles), and 64 (solid squares). The insets show the logarithms of the corresponding frame magnetizations for $L=64$, with lines indicating fits to extract the localization lengths.

ever, they also pointed out that defects in $S=3/2$ chains can cause different behavior (even though $S=1/2$ and $S=3/2$ chains otherwise have the same low-energy properties) in particular that a defect with smaller spin in an $S=3/2$ chain may lead to overscreening, and this in turn could lead either to an effective system corresponding to the periodic chain or possibly to some nontrivial fixed point.¹³ It is hence not clear what kind of behavior to expect in the three-leg ladder with an impurity.

In the open spin-1/2 chain, there is a staggered magnetization decaying as $1/\sqrt{r}$ (times an oscillating function of r) with the distance from an end,¹⁴ which hence would be expected also around an impurity in the three-leg ladder if the impurity is screened. However, the situation may be complicated by the presence of the defect with its screening cloud, which although having total spin 0, can also be associated

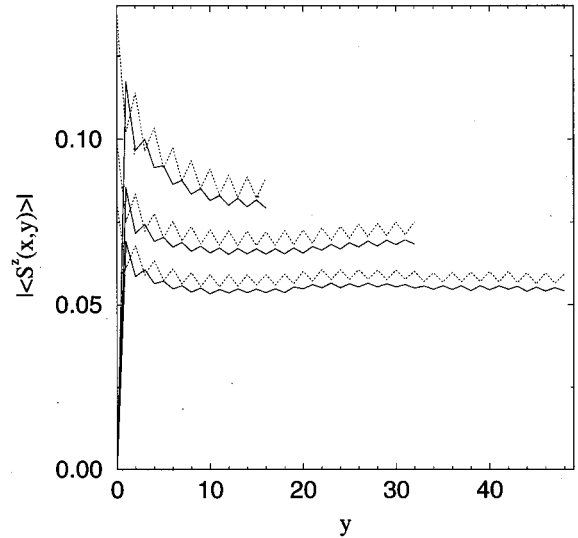


FIG. 4. The magnitude of the magnetization vs the distance from the impurity for three-leg ladders of lengths $L=32$, 64, and 96. Solid lines are for $x=0$ (center chain, with the impurity), and dashed lines for $x=1,3$ (edge chain). For $L=64$ and $L=96$, there are $\approx 5\%$ statistical errors for $y>10$, which affect the overall amplitudes, but not the oscillating behavior.

with a staggered magnetization. Hence, the behavior found in the open spin-1/2 chain would likely only be reproduced at very large distances from the impurity, even if this mapping would indeed be the correct one.

Figure 4 shows our results for the local staggered magnetization $|\langle S^z(x,y) \rangle|$ versus the distance from the impurity for systems with up to 3×96 sites. At long distances, $|\langle S^z(x,y) \rangle|$ is almost flat, and its magnitude decreases as the system size increases. The integrated uniform and staggered magnetizations are shown in Fig. 5. The even-odd oscillations in $I_0(R)$, which are absent for the two-leg ladder, are clearly due to the fact that the rungs have an odd number of sites, so that an effective cancellation of the staggered magnetization can only occur for odd R (with the impurity on the center chain). Nevertheless, as the system size grows, a clear decay of $I_0(R)$ for each R can be seen [for example, the inset shows $I_0(R=10)$ vs the inverse ladder length], consistent with no localized moment as $L \rightarrow \infty$. The integrated staggered magnetization $I_\pi(R)$ grows approximately linearly with R , with a slope which is smaller for the larger systems [in accordance with the flat behavior observed above for $|\langle S^z(x,y) \rangle|$]. The full staggered moment $I_\pi(L/2)$ appears to diverges as $L \rightarrow \infty$, but the divergence is clearly slower than L . If indeed $I_\pi(R) \sim R$, and $I_\pi(L/2) \sim L^\alpha$, with $\alpha < 1$, then $I_\pi(R) \rightarrow 0$ for any R as $L \rightarrow \infty$. However, our results for small R are not of sufficient accuracy to rule out a different behavior very close to the impurity. In any case, the behavior appears to be different from the $1/\sqrt{r}$ decay of the staggered magnetization with distance r from the open end of a spin-1/2 single chain,¹⁴ and hence indicates that the system does not map onto this model. The tendency to spread the induced staggered magnetization evenly over the whole system may indicate a divergent screening length. Further studies are clearly needed to resolve this issue.

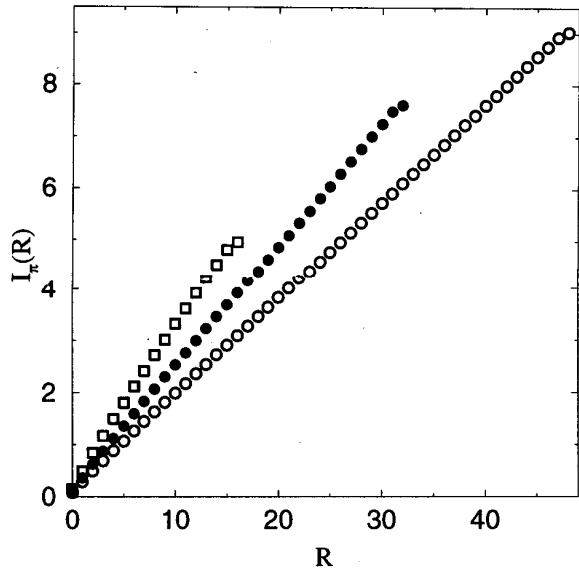
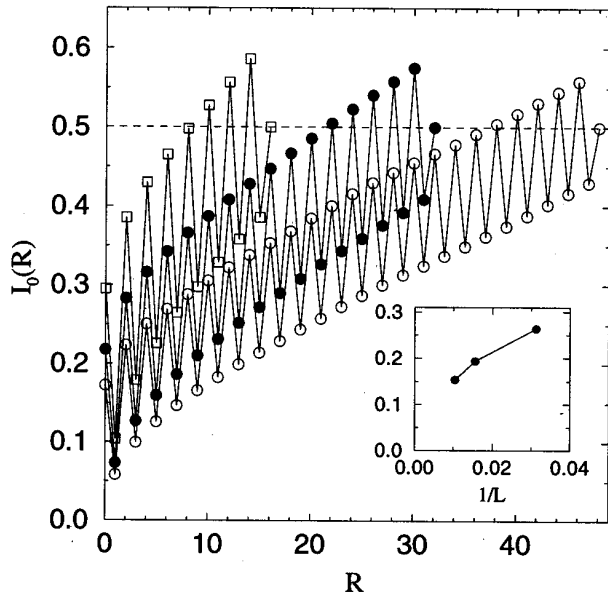


FIG. 5. The integrated uniform (top panel) and staggered (bottom panel) magnetizations vs the distance from the impurity (with R defined in Fig. 1) for three-leg ladders of length $L=32$ (open squares), 64 (solid circles), and 96 (open circles). The inset of the top panel shows $I_0(R=10)$ vs the inverse system size.

C. 2D systems

Effects of an impurity in the 2D Heisenberg model was previously discussed by Bulut *et al.*,¹⁵ on the basis of linear spin-wave theory and exact diagonalization of a 4×4 lattice. It was concluded that the total $S^z = 1/2$ distortion of the order parameter is localized to the close vicinity of the impurity, and that the order is actually enhanced at the site closest to the impurity.

Here we begin by studying the doubly degenerate $S=1/2$ ground state of small periodic square lattices with one spin removed, in the same way as done above for the ladder systems. Figure 6 shows the average magnetization vs distance

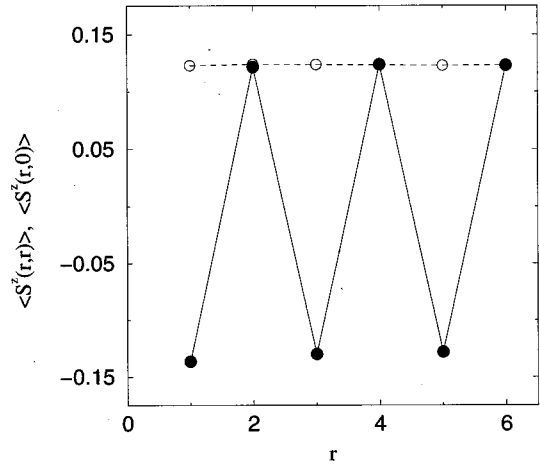


FIG. 6. Site-dependent magnetization of a 2D 12×12 lattice with an impurity at $(x,y)=(0,0)$, along the lines $(r,0)$ (solid circles), and (r,r) (open circles).

from the impurity in the $m^z = -1/2$ sector of a 12×12 lattice. The magnitude of the magnetization is almost independent of the distance. Naively one might expect that this staggered order induced by removing a spin is equal to the sublattice magnetization. This is not the case, however. To see this, we first consider the sublattice magnetization m^+ , which for a rotationally invariant finite system, can be defined as¹⁶

$$m^+/\sqrt{3} = \sqrt{S_\pi/N}, \quad (4)$$

where S_π is the staggered structure factor

$$S_\pi = \frac{1}{N} \sum_{x_1, y_1} \sum_{x_2, y_2} (-1)^{x_1 - x_2 + y_1 - y_2} \langle S^z(x_1, y_1) S^z(x_2, y_2) \rangle. \quad (5)$$

In a lattice with one spin removed the rotational invariance is broken. However, in contrast to the thermodynamic limit broken-symmetry state, the staggered magnetization is not fully locked in the z direction. It is clear that the removal of a single spin from a large system cannot significantly change the average long-distance correlation functions, and hence scaling Eq. (4) to infinite system size should give the correct sublattice magnetization also with an impurity present. The staggered magnetization $|\langle S^z(x, y) \rangle|$ induced by a missing spin (in a finite lattice, and scaling to infinite system size without breaking the symmetry) must therefore be smaller than the true sublattice magnetization m^+ . In Fig. 7 we compare $\sqrt{S_\pi/N}$ calculated on 2D lattices with and without an impurity, and the average

$$m_\pi = \frac{1}{L^2 - 1} \sum_{x, y} |\langle S^z(x, y) \rangle|, \quad (6)$$

of the staggered magnetization of systems with an impurity. Without fluctuations in $S^z(x, y)$ (as would be the case if the symmetry is fully broken and staggered magnetization has locked in the z direction), m_π would be equal to $\sqrt{S_\pi/N}$. The results in Fig. 7 clearly show that there are in fact large fluctuations, since m_π is considerably smaller than $\sqrt{S_\pi/N}$. The dependence of m_π on $1/L$ is close to linear, and scaling

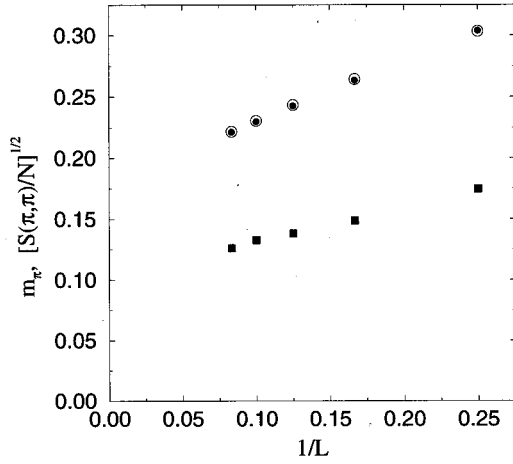


FIG. 7. The staggered structure factor vs inverse system size for $L \times L$ square lattices (solid circles), and with one spin removed (open circles). The solid squares show the induced staggered magnetization averaged over all the sites in a system with one spin removed.

to infinite system size gives $m_\pi \approx 0.11$. $\sqrt{S_\pi/N}$ is only slightly affected by the presence of a static hole, as expected, and scales to a value consistent with the known^{16,17} sublattice magnetization $m^+/\sqrt{3} \approx 0.18$. Hence, there is a factor ≈ 3 relating m_π and the full staggered magnetization in this case.

Figure 8 shows the integrated uniform magnetization $I_0(R)$ for different system sizes. For a given distance R from the impurity, $I_0(R)$ decreases with increasing system size, approaching a finite value as $L \rightarrow \infty$. Quadratic fits used for extrapolations are shown for $R=1$ and $R=2$. The results are considerably lower than those obtained within spin-wave theory.¹⁵ Again, this is clearly due to a rotational reduction, as discussed above. The longitudinal component of the magnetization is only partially directed along the quantization axis used, and the distortion of the longitudinal component is therefore not seen fully in this type of calculation.

In order to study the full effects of an impurity on the antiferromagnetic background, we have to explicitly break the symmetry, so that the longitudinal correlation functions can be directly accessed. Here we achieve this situation by coupling the edges of a system with open boundary conditions to spins which are fixed in an antiferromagnetic configuration. For this Ising-type interaction we arbitrarily choose the same strength J as the Heisenberg interaction among the interior spins. At the center of the system, the staggered edge spins have an effect similar to a staggered field with a strength that vanishes as the system size grows. Comparing results for this system with one where the center spin is removed gives a direct measure of the distortion of the antiferromagnetic background due to an impurity. The two lattices are illustrated in Fig. 9.

First, in order to verify that this method gives the known value of the staggered magnetization at the center of the lattice without an impurity, we studied such systems with up to 25×25 spins. Extrapolating the expectation value $\langle S_0^z \rangle$, with $i=0$ being the center spin, gives a sublattice magnetization ≈ 0.305 , which is in good agreement with previous calculations.^{16,17}

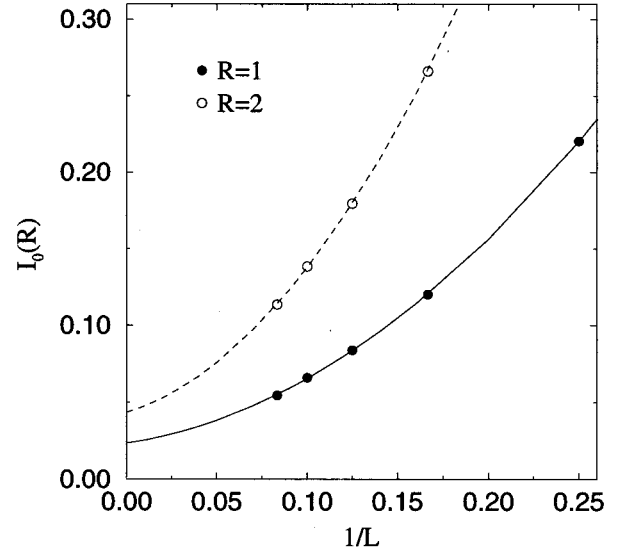
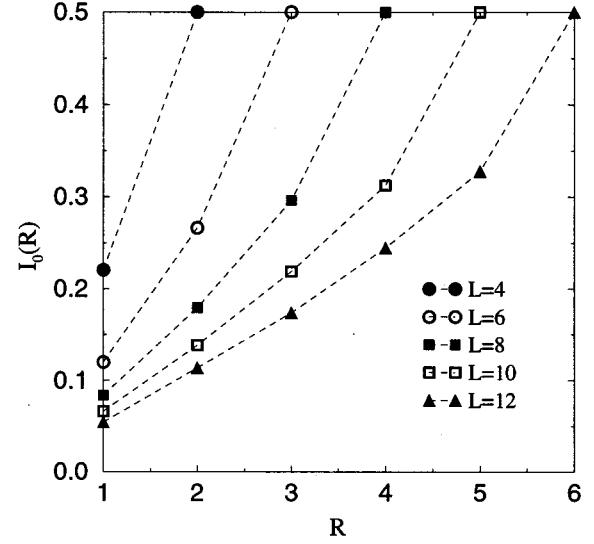


FIG. 8. Upper panel: Integrated moment vs R for 2D lattices of different sizes. Lower panel: Finite-size scaling for $R=1$ and $R=2$. The curves are quadratic fits to the QMC results.

We next define the distortion due to an impurity as

$$\langle S_i^z \rangle_\Delta = \langle S_i^z \rangle_I - \langle S_i^z \rangle_0, \quad (7)$$

where $\langle S_i^z \rangle_I$ is the expectation value calculated with the center spin removed, and $\langle S_i^z \rangle_0$ is the results for the intact lattice. We use a sign convention such that $\langle S_i^z \rangle_\Delta > 0$ for the center spin, so that it measures the *reduction* of the magnetization in the presence of the impurity. The QMC results for sites close to the impurity are in good quantitative agreement with the results of linear spin-wave theory presented by Bulut *et al.*¹⁵ In particular, the staggered order at the site closest to the impurity is enhanced. For the largest system studied here ($L=25$), the enhancement is 0.0086(4), whereas linear spin-wave theory gives 0.0107.¹⁵ For all other distances the staggered magnetization is reduced by the impurity, both in spin-wave theory and our present numerical calculations.

Figure 10 shows the uniform and staggered frame magnetizations, which are defined as in Eqs. (2a) and (2b), with

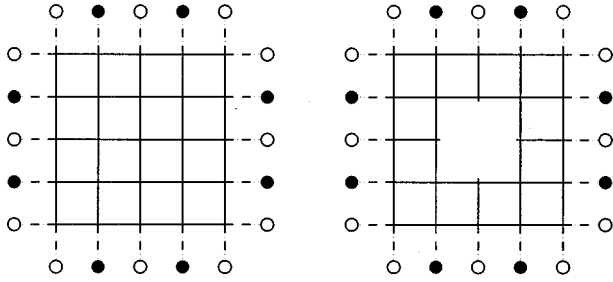


FIG. 9. Lattices used to study systems with broken symmetry. The open and solid circles indicate up and down edge spins which are coupled to the 2D Heisenberg antiferromagnet by Ising couplings (indicated by dashed lines).

$\langle S_i^z \rangle_\Delta$ replacing $\langle S_i^z \rangle$. $M_\pi(R)$ is positive for all R which with our definition means that the averaged staggered magnetization on each frame is reduced by the impurity. Both $M_0(R)$ and $M_\pi(R)$ decay exponentially as R increases, with a localization length ≈ 1.5 lattice spacings.

We can now relate these results to those obtained above without the symmetry-breaking boundaries. The extrapolations shown in Fig. 8 give integrated magnetizations $I_0(1)=0.024$ and $I_0(2)=0.043$. With the staggered boundaries, the data shown in Fig. 8 give $I_0(1)=0.076$ and $I_0(2)=0.135$. Hence, the ratio $I_0(2)/I_0(1) \approx 1.8$ in both cases, but the amplitudes differ by a factor ≈ 3 , which within our numerical accuracy is equal to the factor found above relating the impurity-induced staggered z magnetization to the full sublattice magnetization.

The difference between the localized uniform magnetization induced around an impurity in the 2D case and the moment formed in the two-leg ladder is that the former is always aligned in the direction of the antiferromagnetic

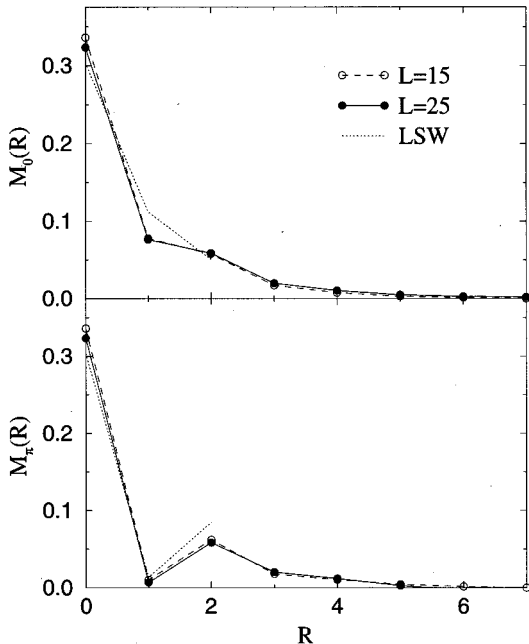


FIG. 10. Uniform (top) and staggered (bottom) magnetization differences within frames at distance R from the lattice center, compared with some of the linear spin-wave (LSW) results by Bulut *et al.*¹⁵

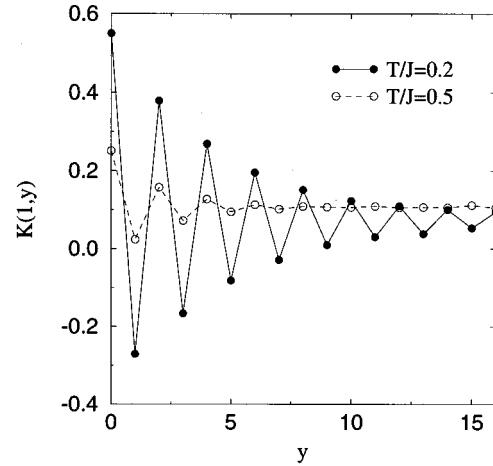


FIG. 11. The Knight shift vs the distance from the impurity in a three-leg ladder with $L=32$ at two different temperatures.

moment. The profound difference between these cases is most clearly seen by considering two well separated impurities on different sublattices. In the two-leg ladder, the corresponding moments can both align along the field in any direction, whereas in a large but finite 2D system the magnetization associated with a single impurity can align with the field, but aligning the second one would require twisting the staggered magnetization in the neighborhood of the impurity. Hence, the term *free* local moment is appropriate only in the context of gapped systems.

III. FINITE-TEMPERATURE KNIGHT SHIFT

The NMR Knight shift K is proportional to the local susceptibility of the electrons close to the nucleus under study. For a strictly on-site hyperfine coupling, K is proportional to the susceptibility of a single spin to a uniform field, and we here defined K accordingly:

$$K(\mathbf{r}) = \int_0^\infty d\tau \sum_i \langle S_i^z(\tau) S_i^z(0) \rangle = \beta \sum_i \langle S_r^z S_i^z \rangle. \quad (8)$$

In a system with impurities, the NMR line shape will reflect the distribution of Knight shifts in the system, and is hence an important probe for studying impurity effects. As an example, the end effects predicted by Eggert and Affleck for the spin-1/2 chain¹⁴ were recently confirmed experimentally in the quasi-1D compound Sr_2CuO_3 by Takigawa *et al.*,¹⁸ and also allowed for an accurate determination of the important hyperfine form factor.

For the two-leg ladder, a divergence of K would be expected in view of the localized moment created by the impurity. However, as discussed above, the induced staggered moment is considerably larger than the uniform moment at low temperatures, which translates to an oscillating behavior also for the Knight shift. For a given T , $K(r \rightarrow \infty)$ approaches the bulk susceptibility χ . The sign of K is positive for all \mathbf{r} at high temperatures. At low temperatures it is negative for sites on the same sublattice as the impurity. Not surprisingly, this behavior is observed also for the three-leg ladder and the 2D system. Figure 11 shows results for the three-leg ladder at two temperatures.

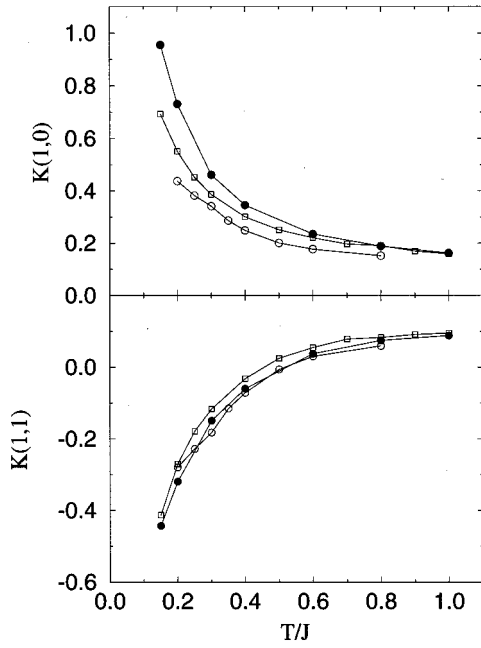


FIG. 12. The temperature dependence of the Knight shift at two sites close to an impurity for a 12×12 plane (open circles), a two-leg ladder of length $L=64$ (solid circles), and a three-leg ladder of length $L=32$ (open squares).

For a spin-1/2 chain with open boundaries, Eggert and Affleck predicted a $T \rightarrow 0$ local susceptibility (Knight shift) which increases as \sqrt{r} with the distance r from the boundary. A finite temperature exponentially suppresses the increase, resulting in a maximum that is shifted towards the interior of the chain as $T \rightarrow 0$. This was confirmed numerically.¹⁴ Our results for the three-leg ladder with an impurity do not exhibit the shift of the maximum, even at considerably lower temperatures than those shown in Fig. 11. This is another indication that the system does not map onto a spin-1/2 chain with a screened defect.

Figure 12 shows the temperature dependence of $K(1,0)$ and $K(1,1)$ for all the systems we have studied. In the temperature regime considered the behavior is similar for all systems, with the strongest growth exhibited by the two-leg ladder, for which a divergence is clearly expected in view of the existence of a localized staggered moment (the divergence will occur at all sites, but the prefactor decays exponentially with the distance from the impurity). If the picture of a renormalization to an open spin-1/2 chain holds for the three-leg ladder, the low-temperature Knight shift should converge to a value $\sim \sqrt{R}$. As already discussed, none of our numerical results have shown this behavior. In the 2D case, we expect a divergence of K at all distances in view of the staggered moment resulting from the long-range order of the system at $T=0$.

IV. SUSCEPTIBILITY FOR A FINITE IMPURITY CONCENTRATION

Another quantity of experimental interest as a probe of the effects of impurities is the magnetic susceptibility. In this case, in order to determine the low-temperature behavior of the susceptibility, one must treat a finite concentration of impurities taking into account their interaction. The effects

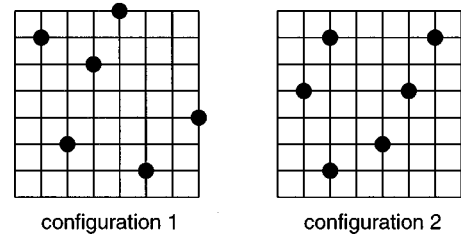


FIG. 13. The two impurity configurations for which the susceptibility was calculated. The solid circles indicate lattice sites without spins (nonmagnetic impurities).

of a finite concentration of nonmagnetic impurities on a two-leg ladder have recently been extensively studied. As we have seen, a local moment is formed around the impurity along with an induced staggered magnetization which experimentally decays on a length set by the spin gap of the ladder. Fukuyama *et al.*²¹ showed that for a finite impurity concentration, while the amplitude of the staggered magnetization was inhomogeneous due to the random distribution of impurities, there was a persistence in their staggered spin correlations leading to an enhanced $q = (\pi, \pi)$ susceptibility. Motome *et al.*¹⁹ used exact diagonalizations of small clusters and variational calculations to show that antiferromagnetic correlations were enhanced in an impurity doped two-leg ladder. They also found low-lying excited states in the spin gap, suggesting that a small but finite concentration of impurities reduces or eliminates the spin gap. Similarly, Martins *et al.*²⁰ found that impurities induced low-lying excited states which are seen in the dynamic magnetic structure factor of a spin-gapped system. They noted that these states arose when nonmagnetic impurities doped into a spin-gapped system created local moments which coupled with a random distribution of strengths. These authors also found enhanced antiferromagnetic correlations in the vicinity of a nonmagnetic impurity for a dimerized $S=1/2$ chain (to model CuGeO_3), a system which also has a spin gap. Sigrist and Furusaki²² noted that nonmagnetic impurities doped into a two-leg Heisenberg ladder create local spin-1/2 degrees of freedom which interact via the spin-liquid background. As the temperature is lowered, correlations then develop among the impurity moments and the system renormalizes into coupled clusters with coherent staggered correlations on a long length scale.

All of these treatments rely on the existence of local moments formed around the impurities, which are coupled via the exponential spin-spin correlations in the spin liquid. Thus the behavior of an impurity doped two-leg ladder should be different from the 2D lattice, for which we have argued that the induced localized magnetization around the impurity does not correspond to a free moment, but is always aligned with the local staggered order (although the system is not antiferromagnetically ordered at finite T , the staggered correlation length at low T is much larger than the localization length of the distortion found in the previous section). Here we contrast the uniform susceptibility of a 2D lattice and a two-leg ladder.

We begin by showing results for the temperature dependence of the uniform susceptibility χ of a periodic 8×8 Heisenberg model with six randomly placed impurities. Figure 13 shows two ‘‘typical’’ impurity configurations for

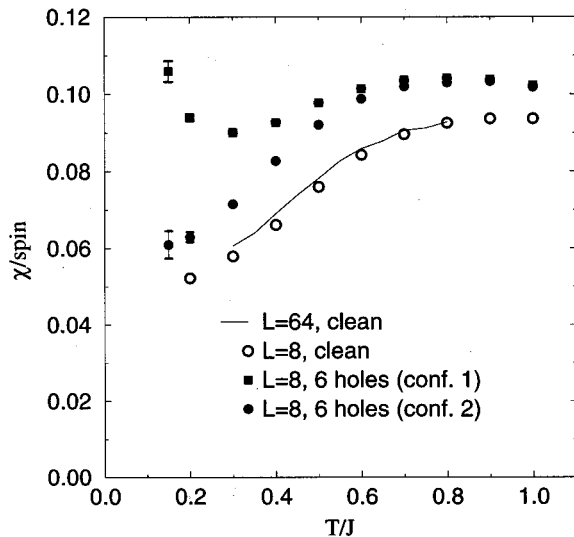


FIG. 14. The uniform magnetic susceptibility vs temperature for the hole configurations shown in Fig. 1, and for pure systems.

which we have carried out simulations. The temperature dependence of χ for these configurations are shown in Fig. 14, along with results for a pure system of the same size. Pure system results for a lattice of 64×64 sites are also shown, to give an idea about the finite-size effects. The two impurity configurations give strikingly different susceptibilities; for configuration 1, χ appears to diverge at low T , whereas configuration 2 has a χ similar to the clean system, although somewhat enhanced.

The reason for the different behavior of χ of the two configurations can be readily understood qualitatively. As already discussed, the total spin S of the ground state of a Heisenberg model on a bipartite lattice depends on the difference of the number of spins on the two sublattices. If there are N_A and N_B spins in sublattices A and B , respectively, the ground state has $S = \frac{1}{2} |N_A - N_B|$.⁸ Hence, in the case under consideration here, the ground state is a singlet only if there are equal numbers of impurities on the two sublattices, and has a finite spin if this is not the case. If the ground state is not a singlet, one of course gets a Curie behavior of χ at low T , whereas if $S=0$, χ may be finite or decay to zero as $T \rightarrow 0$, depending on if there is a gap in the spectrum or not. Inspecting the hole configurations in Fig. 13, one indeed finds that configuration 1 has two holes in one sublattice and four in the other one, whereas configuration 2 has three holes in each sublattice. This explains the qualitatively different susceptibilities of these lattices. The nondivergent behavior in the $S=0$ case is another indication that inert impurities in 2D are not associated with localized free moments. Such moments in a finite system with $S=0$ would lead to an increase in χ before the eventual activated behavior caused by the finite-size gap, approaching a true $T \rightarrow 0$ divergence as $L \rightarrow \infty$.

For a system with N sites and a random impurity concentration p , the expected difference of the number of holes on sublattices A and B is $\propto \sqrt{pN}$. Hence, the Curie part of the susceptibility scales as $1/\sqrt{N}$, and vanishes as $N \rightarrow \infty$. Furthermore, the temperature at which the Curie behavior will be seen decreases with the system size, since the ground state

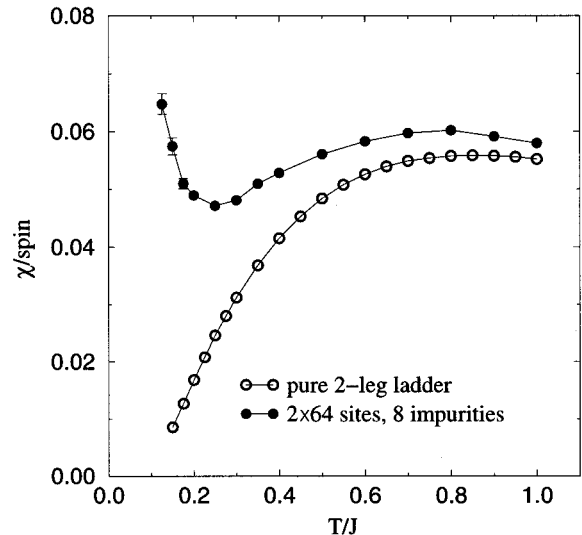


FIG. 15. The uniform magnetic susceptibility vs temperature for a pure two-leg ladder with 2×64 sites, and one of the same size where eight spins have been removed. Numbering the sites of the chains 1–64 and 65–128, the removed spins are at sites 1, 22, 31, 46, 70, 79, 99, 120, so that there are equal numbers of spins on each sublattice, and the ground state therefore is a singlet.

has a zero measure in the partition function in the thermodynamic limit, and its spin therefore is irrelevant. Of course, if the impurity concentration is sufficiently large to cause the system to break up into disconnected pieces, there will always be a Curie component arising from small pieces containing an odd number of spins. This contribution survives the $N \rightarrow \infty$ limit, but does not scale linearly with the impurity concentration in 2D.

Random impurities in a one-dimensional system, such as a single chain or a ladder, cut the system into disconnected pieces, and the ones with $N_A - N_B \neq 0$ give rise to a Curie contribution to the susceptibility which grows with p much more rapidly than in 2D. However, as reviewed above, for ladders with an even number of legs, a more interesting contribution is expected, due to localized moments which are induced around impurities in spin-gapped systems. In order to observe the effects of such localized moments we have simulated a 2×64 site ladder with eight impurities (corresponding to a concentration $p = 6.25\%$) in a configuration such that the system remains in one connected piece. Furthermore, we choose the configuration such that $N_A = N_B$, so that the ground state is a singlet and therefore any divergent behavior is due to localized moments forming around the impurities. The temperature dependence for χ in such a system is shown in Fig. 15, along with the susceptibility of a pure Heisenberg ladder. The pure system shows the activated behavior typical for a gapped system. For this case (equal rung and chain couplings), the gap $\Delta \approx 0.50J$. In contrast, the system with impurities show a minimum in χ at $T \approx 0.25J$, and then a sharp increase for lower temperatures. Since the ground state is a singlet when $N_A = N_B$, and the system is finite, the uniform susceptibility will eventually vanish as $T \rightarrow 0$. In the thermodynamic limit it will show a true divergence. Free localized moments would give a Curie behavior, but since the system consists of a single connected lattice the induced moments will have an effective interaction which

depends on the distances between the impurities. As discussed by Sigrist and Furusaki,²² this leads to a nontrivial divergent behavior.

V. SUMMARY

From these calculations, we have seen that a single nonmagnetic impurity induces a local moment on a two-leg ladder but not on a three-leg ladder or on a 2D lattice. The induced staggered magnetization around the impurity on a two-leg ladder has a localization length $\xi_\pi \approx 3.2$ set by the spin-gap correlation length of the pure ladder. A staggered magnetization is also induced on a three-leg ladder, but its amplitude at a given distance from the impurity decays strongly with increasing system size L . Nevertheless, the staggered magnetization integrated over the whole ladder appears to diverge as $L \rightarrow \infty$. We have discussed the possibility of the system mapping onto a spin-1/2 chain with a screened defect (which in turn corresponds to an open chain), but the behavior found does not appear to support this picture. On finite 2D lattices, the induced staggered magnetization remains finite at all distances from the impurity as the system size grows, reflecting the long-range order in the ground state of the pure system. The sublattice magnetization seen in this case (in the direction of the quantization axis used) is smaller than the full sublattice magnetization, which is seen only if the symmetry is further broken by a staggered field. There is an exponentially decaying distortion of the sublattice magnetization in the neighborhood of the impurity. Our numerical results for the magnitude of this distortion are in good agreement with previous spin-wave calculations.¹⁵

We have also discussed the NMR Knight shift, which depends on the temperature and the distance from the impurity in a manner reflecting the behavior of the staggered mag-

netization at $T=0$. It would clearly be interesting to experimentally search for these effects in the NMR line shape in two- and three-leg ladder materials, as was recently done by Takigawa *et al.* for the single-chain material Sr_2CuO_3 .¹⁸

The uniform susceptibility of two-leg ladders in the presence of a finite concentration of impurities has been discussed in detail recently.²² Here we have presented numerical results confirming that the localized moments in this gapped system cause a divergent susceptibility at low temperatures. We have also shown that this does not occur in the gapless 2D system, for which the moment introduced by an impurity is not free, but aligned with the local staggered order.

An interesting system in which to study the effects of nonmagnetic impurities would be a 2D system that can be tuned through a quantum critical point. The Heisenberg bilayer, with interlayer and intralayer couplings J_2 and J_1 , respectively, is critical at $(J_2/J_1)_{\text{critical}} \approx 2.5$.²³ Nonmagnetic impurities should hence be associated with free local moment only for J_2/J_1 larger than this value, with the localization length diverging at $(J_2/J_1)_{\text{critical}}$.

Note added in proof. Zn impurity effects on the NMR line shape of the type we have discussed here, in Sec. III, were recently observed in the two-leg ladder compound SrCu_2O_3 by Fujiwara *et al.*²⁴

ACKNOWLEDGMENTS

This work was supported by National Science Foundation under Grant Nos. DMR-9520776 (A.W.S. and E.D.) and DMR-9527304 (D.J.S.). The QMC calculations were carried out at the Supercomputer Computations Research Institute (SCRI) at Florida State University.

*Present address: Department of Physics, University of Illinois at Urbana-Champaign, 1110 West Green Street, Urbana, Illinois 61801.

¹A. V. Mahajan, H. Alloul, G. Collins, and J. F. Marucco, Phys. Rev. Lett. **72**, 3100 (1994).

²M. Azuma, Y. Fujishiro, M. Takano, M. Noharo, and H. Takagi, Phys. Rev. B **55**, R 8658 (1977); M. Azuma, M. Takano, T. Ishida, and K. Okuda (unpublished).

³N. Nagaosa and T.-K. Ng, Phys. Rev. B **51**, 15 588 (1995).

⁴A. W. Sandvik and J. Kurkijärvi, Phys. Rev. B **43**, 5950 (1991); A. W. Sandvik, J. Phys. A **25**, 3667 (1992).

⁵D. C. Handscomb, Proc. Camb. Philos. Soc. **58**, 594 (1962); **60**, 116 (1964); D. H. Lee, J. D. Joannopoulos, and J. W. Negele, Phys. Rev. B **30**, 1599 (1984).

⁶M. Suzuki, S. Miyashita, and A. Kuroda, Prog. Theor. Phys. **58**, 1377 (1977); J. E. Hirsch, R. L. Sugar, D. J. Scalapino, and R. Blankenbecler, Phys. Rev. B **26**, 5033 (1982).

⁷A. W. Sandvik, A. V. Chubukov, and S. Sachdev, Phys. Rev. B **51**, 16 483 (1995); A. W. Sandvik and D. J. Scalapino, *ibid.* **53**, R526 (1996); O. A. Starykh, A. W. Sandvik, and R. R. P. Singh, *ibid.* **55**, 14 953 (1997).

⁸E. H. Lieb and D. C. Mattis, J. Math. Phys. (N.Y.) **3**, 749 (1962).

⁹E. Dagotto, J. Riera, and D. J. Scalapino, Phys. Rev. B **45**, 5744 (1992).

¹⁰S. R. White, R. M. Noack, and D. J. Scalapino, Phys. Rev. Lett. **73**, 886 (1994).

¹¹T. Barnes and J. Riera, Phys. Rev. B **50**, 6817 (1994).

¹²B. Frischmuth, S. Haas, G. Sierra, and T. M. Rice, Phys. Rev. B **55**, R3340 (1997).

¹³S. Eggert and I. Affleck, Phys. Rev. B **46**, 10 866 (1992).

¹⁴S. Eggert and I. Affleck, Phys. Rev. Lett. **75**, 934 (1995).

¹⁵N. Bulut, D. Hone, D. J. Scalapino, and E. Y. Loh, Phys. Rev. Lett. **62**, 2192 (1989).

¹⁶J. D. Reger and A. P. Young, Phys. Rev. B **37**, 5978 (1988).

¹⁷K. J. Runge, Phys. Rev. B **45**, 7229 (1992); B. B. Beard and U.-J. Wiese, Phys. Rev. Lett. **77**, 5130 (1996); A. W. Sandvik, Phys. Rev. B (to be published).

¹⁸M. Takigawa, N. Motoyama, H. Eisaki, and S. Uchida, Phys. Rev. B **55**, 14 129 (1997).

¹⁹Y. Motome, N. Katoh, N. Furukawa, and M. Imada, J. Phys. Soc. Jpn. **65**, 1949 (1996).

²⁰G. B. Martins, E. Dagotto, and J. A. Riera, Phys. Rev. B **54**, 16 032 (1996).

²¹H. Fukuyama, N. Nagaosa, M. Saito, and T. Tomimoto, J. Phys. Soc. Jpn. **65**, 2377 (1996).

²²M. Sigrist and A. Furusaki, J. Phys. Soc. Jpn. **65**, 2385 (1996); see also, H. J. Mikeska, U. Neugebauer, and U. Schollwöck, Phys. Rev. B **55**, 2955 (1997).

²³A. W. Sandvik and D. J. Scalapino, Phys. Rev. Lett. **72**, 2777 (1994).

²⁴N. Fujiwara, H. Yasuoka, Y. Fujishiro, M. Azuma, and M. Takano (unpublished).